X-ray diffraction and impedance spectroscopy studies of lithium manganese oxide spinel

M. Kopeć[a], D. Lisovytskiy[b], M. Marzantowicz[a], J.R. Dygas[a,*],
F. Krok[a], Z. Kaszkur[b], J. Pielaszek[b]

[a] *Faculty of Physics, Warsaw University of Technology, Koszykowa 75, 00-662 Warszawa, Poland*
[b] *Institute of Physical Chemistry, Polish Academy of Sciences, Kasprzaka 44/52, 01-224 Warszawa, Poland*

Available online 29 March 2006

Abstract

Phase transition in lithium manganese oxide spinel synthesized by sol–gel technique and in samples prepared from commercially available powders of $LiMn_2O_4$ (Alfa-Aesar and Sigma–Aldrich) was investigated. In addition to the standard impedance measurements and the X-ray diffraction in Bragg–Brentano geometry, simultaneous measurements of impedance spectrum and X-ray pattern in non-focusing geometry were performed in the temperature range between -25 and $+100\,^\circ\text{C}$. Correlation between the XRD profile parameters and the electrical conductivity was evidenced. Spinel synthesized by the sol–gel technique and heat-treated at $800\,^\circ\text{C}$ as well as samples prepared from Alfa-Aesar powder exhibited a distinctive phase transition from cubic to orthorhombic structure upon cooling below room temperature. Structural transition was visible in the X-ray pattern as splitting of the $4\,0\,0$ reflection of cubic structure, and was accompanied by a decrease of conductivity by a factor of about 10. In the sample prepared from powder supplied by Sigma–Aldrich the phase transition was not complete even upon cooling to $-25\,^\circ\text{C}$, and no stepwise change of conductivity was observed. Differences in behavior of the spinel samples can be related to the presence of additional phases (Mn_3O_4 or Li_2MnO_3), which were found in commercial powders, whereas the sol–gel synthesized samples were single phase.
© 2006 Elsevier B.V. All rights reserved.

Keywords: Lithium manganese spinel; X-ray diffraction; Impedance spectroscopy; Structural phase transition

1. Introduction

By virtue of the high cell voltage, large reversible capacity, low cost and low toxicity, lithium manganese oxide spinels are promising alternative to $LiCoO_2$, currently used in the lithium-ion batteries as cathode material [1–3]. The crystal structure of the spinel $LiMn_2O_4$ consists of cubic close-packed oxide ions with manganese ions in half of the octahedral sites and lithium ions in one eighth of the tetrahedral sites formed by the oxide lattice [1,2]. In the stoichiometric spinel, manganese ions coexist in two valence states Mn^{3+} and Mn^{4+} in equal proportions. The electrical conductivity is due to thermally activated hopping of electrons between neighbor mixed valence manganese ions [4]. $LiMn_2O_4$ spinel undergoes a reversible phase transition upon cooling and heating at temperatures close to room temperature. The crystal structure above the transition temperature is cubic (space group Fd-$3m$). The low temperature phase was initially considered to be tetragonal [5–7], and the phase transition was attributed to a long range ordering of the local Jahn–Teller distortion of $Mn^{3+}O_6$ octahedra [6]. Later it was concluded that at temperatures below the phase transition there was a single phase of the orthorhombic symmetry (space group *Fddd*) [8–11]. Observations of extra reflections in electron diffraction and neutron powder diffraction at low temperature led to conclusion that the orthorhombic distortion of the cubic spinel structure was associated with partial charge ordering on manganese sites [9,10]. The partially charge ordered structure was envisaged as columns of Mn^{3+} type ions running along the $[0\,0\,1]$ direction, which are surrounded by Mn^{4+} ions. Ordering of electronic charge was invoked to explain the decrease of conductivity, which accompanies the phase transition from cubic to orthorhombic symmetry [7,10]. The observed drop of conductivity may be more or less sharp, depending on the method of preparation and the deviation from the stoichiometric $LiMn_2O_4$ composition [12,13]. It was observed that oxygen deficiency, which may vary with the sample thermal history, is the major factor determining the occurrence of the phase transition and the actual value of the transition temperature [14–16].

* Corresponding author. Tel.: +48 22 6608213; fax: +48 22 6282171.
E-mail address: jrdygas@if.pw.edu.pl (J.R. Dygas).

From the point of view of possible application of Li–Mn–O spinels in lithium-ion batteries, it is of crucial importance to understand the effect of phase transition on the electrical properties. Presence of the impurity phases can influence the course of phase transition of the main spinel phase. Studies of the electrical and structural properties of lithium manganese oxide spinels obtained by the sol–gel method have been reported in our previous publications [17–19]. It was observed that the samples of nominal composition close to $LiMn_2O_4$, when heat-treated at 800 °C, were single phase stoichiometric spinel in which the phase transition from cubic to orthorhombic structure took place below the room temperature. Simultaneous measurements of the conductivity and the X-ray diffraction pattern during the phase transition were conducted in a specially developed experimental setup that combined an impedance analyzer and an X-ray diffractometer equipped with a position sensitive detector [19]. In the present work the main aim was to compare electrical and structural properties of samples prepared from the commercially available $LiMn_2O_4$ powder (supplied by Alfa-Aesar and Sigma–Aldrich) with those of the spinels synthesized by the sol–gel technique. The commercial materials were of the grade recommended for application in batteries and the information on their composition is presented as provided by suppliers. For both types of samples, the impedance measurements and the X-ray diffraction studies were conducted, either separately or simultaneously, in course of the stepwise increase and subsequently the stepwise decrease of temperature in the region of the phase transition. This investigation is intended to lay the ground for building a prototype electrochemical cell based on lithium ion polymer electrolyte and $LiMn_2O_4$ as cathode material.

2. Experimental

High purity starting reagents $LiNO_3$ and $Mn(CH_3COO)_2 \cdot 4H_2O$ (Aldrich 99.99%) were used for synthesis of lithium manganese oxide by the sol–gel method. Preparation procedure has been described elsewhere [17,20]. Pellets formed from powders calcined in air at 300 °C were sintered at 800 °C for 24 h and rapidly cooled (by taking out of the furnace). Two samples obtained by the sol–gel method were used in this study: stoichiometric $LiMn_2O_4$ and slightly lithium substituted $Li_{1.005}Mn_{1.995}O_4$. Commercially available powders of $LiMn_2O_4$ were purchased from Alfa-Aesar (according to supplier: purity 99.5% metals basis; −325 mesh powder; assay: Li 3.46 wt.%, Mn 60.66 wt.%; analysis: Al 0.05 wt.%, Mg 0.01 wt.%; Fisher size 9.44 μm, major XRD pattern matches PDF# 35–782 cubic) and from Sigma–Aldrich (according to supplier: electrochemical grade; 61.5% Mn by titration with $KMnO_4$; 4.9 wt.% loss on ignition at 1100 °C for 1 h; XRD conforms to standard pattern; blackish blue powder; particle size 93 wt.% +60 mesh). Powders as received were pressed into pellets of 10 mm diameter and about 1 mm thickness. Serious difficulties resulting from splitting and cracking were encountered while forming pellets by uniaxial pressing, particularly from powder supplied by Sigma–Aldrich. Pellets that appeared to be homogenous were subsequently isostatically pressed at 350 MPa and sintered in air at 800 °C for 24 h and rapidly cooled. Microstructure of sintered materials was examined by scanning electron microscope (Zeiss Leo 1430 VP) on fractured surfaces without application of additional conductive thin film (Fig. 1). Average grain size was evaluated by counting the number of grain
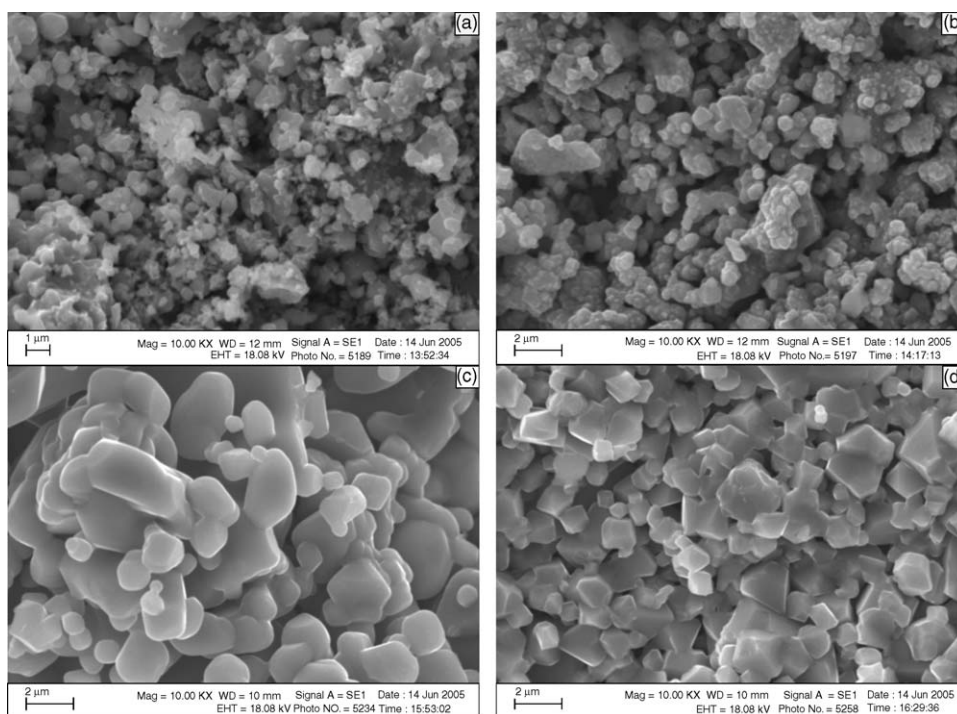

Fig. 1. SEM micrographs of surfaces of fractured pellets sintered at 800 °C from powders obtained by the sol–gel method: (a) $LiMn_2O_4$, (b) $Li_{1.005}Mn_{1.995}O_4$; or from commercially available powders supplied by: (c) Alfa-Aesar, (d) Sigma–Aldrich.
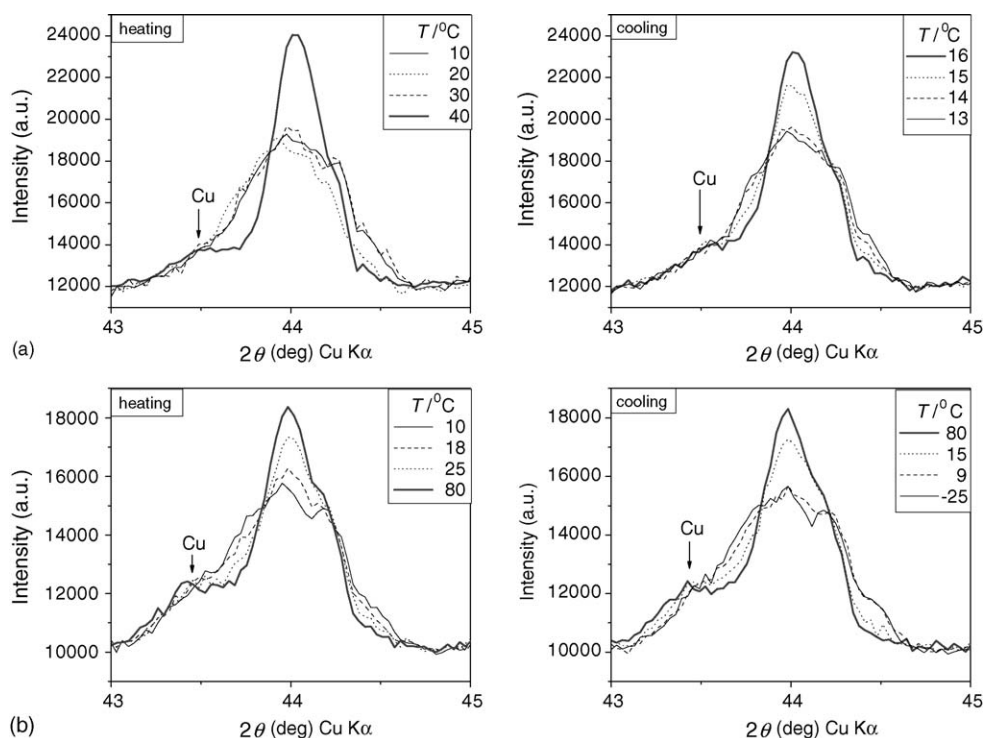
Fig. 2. XRD pattern near the 4 0 0 reflection recorded at various temperatures during heating and cooling of spinel samples obtained by the sol–gel method and sintered at 800 °C: (a) $LiMn_2O_4$, (b) $Li_{1.005}Mn_{1.995}O_4$.

boundaries crossing sections of a straight line drawn on SEM picture.

For simultaneous measurement of impedance and X-ray diffraction pattern thin copper electrodes were sputtered on the polished surfaces of the pellets. Copper was found to be the most convenient electrode in respect to the other metals tested (Pt and Au), because it offers low absorption of Cu Kα radiation and has low resistance. As shown in Fig. 2, the 1 1 1 reflection from Cu layer does not significantly obscure the 4 0 0 reflection from $LiMn_2O_4$ spinel (reflection used to trace the phase transition). Some measurements of impedance were also made with sputtered gold electrodes.

Powder X-ray diffraction was performed on a standard Siemens D5000 diffractometer with Bragg-Brentano geometry and Ni filtered Cu Kα radiation. Data were collected at 50 and at −25 °C (or −4 °C) in the 2θ range from 10° to 90° with narrow step of 0.02°. The Rietveld refinement was made for structure and phase identification using program Fullprof [21] and starting structural data from JCPDS and ICSD databases. The average crystallite size was estimated from the integral width of the 2 2 2 reflection of the cubic spinel using the Scherrer formula. Value of the integral width was obtained using PeakFit software to fit analytical functions of the Pearson VII type to the particular reflection.

Impedance measurements in the frequency range from 10 MHz to 0.1 Hz were made with Solartron 1260 coupled to Keithley 428 current amplifier at temperatures between −60 and +100 °C. Simultaneous measurements of the impedance spectrum and the X-ray diffraction pattern in the non focusing geometry were performed in the temperature range from −25 to +100 °C. In both types of measurement the sample was placed in a custom designed holder heated or cooled by Peltier elements. Temperature was changed stepwise. In the temperature range above and below the expected temperature of the phase transition, the temperature step of 10 or 5 °C was used, whereas in the vicinity of the phase transition temperature the step was smaller (1 °C). Before each measurement the temperature was allowed to stabilize for at least 10 min. Automated set-up combining the X-ray diffractometer with INEL CPS-120 curved position sensitive detector and an AutoLab potentiostat PGSTAT30 with frequency response analyzer FRA2 was used for in situ experiments [19]. Detection of impedance drift was used to investigate the phase transition at isothermal conditions until the system reached steady state. Measurements of the impedance spectrum and the X-ray pattern were automatically repeated at the same temperature when the calculated drift of impedance exceeded the specified limit (typically 1% over period of 15 min). Similar drift detection procedure has been successfully applied in the investigation of phase transition phenomena in oxide ion conducting ceramics [22] and polymer electrolytes [23].

Separate analysis of the 4 0 0 reflection of the cubic spinel, which undergoes splitting into 4 0 0, 0 4 0, 0 0 4 upon orthorhombic distortion, was performed for tracing the phase transition in the X-ray pattern collected with the position sensitive detector. Due to limited resolution of the position sensitive detector and a large scatter of intensity, it was not feasible to perform fitting of a combination of diffraction peaks originating from cubic and orthorhombic phases of the spinel. Therefore, a single peak, which approximated the superposed reflections from spinel, and an adjacent peak due to the 1 1 1 reflection from the
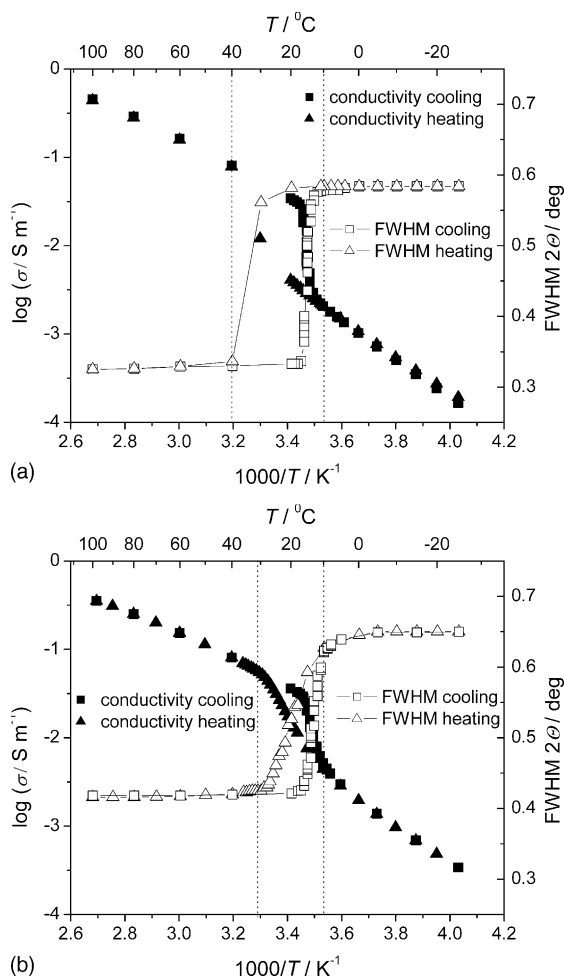
Fig. 3. Temperature dependence of the conductivity and the full width at half maximum (FWHM) of the 4 0 0 reflection for spinel powders synthesized by sol–gel method and sintered at 800 °C: (a) $LiMn_2O_4$, (b) $Li_{1.005}Mn_{1.995}O_4$. Results of impedance measurements simultaneous with acquisition of the X-ray pattern. Multiple data points at a given temperature in the cooling run correspond to measurements in isothermal mode enforced by the impedance drift detection algorithm.

Cu layer, were fitted to the X-ray diffraction pattern near 44° 2θ. Full width at half maximum (FWHM) of the fitted peak was used as a parameter quantifying progress of the phase transition between cubic and orthorhombic structure.

3. Results and discussion

Stoichiometric $LiMn_2O_4$ and slightly Li substituted $Li_{1.005}Mn_{1.995}O_4$ spinels obtained by sol–gel method and heat-treated at 800 °C exhibited phase transition from cubic to orthorhombic structure upon cooling below room temperature. The transition was evidenced by splitting of the 4 0 0 X-ray reflection (Fig. 2) and by anomalies in the temperature dependence of conductivity (Fig. 3). In the case of stoichiometric $LiMn_2O_4$, the conductivity decreased by a factor of about 10 during measurements with impedance drift detection, which caused repetitions of measurements in isothermal mode for a period between 2 and 6 h at consecutive temperatures: 16, 15, 14 and 13 °C (Fig. 3a). During the phase transformation, changes of

the conductivity were well correlated with changes of the shape of the X-ray diffraction pattern near the 4 0 0 reflection, which are presented also in Fig. 2a. There is clear distinction between the single 4 0 0 peak observed at temperatures above 20 °C and the broad intensity maximum seen at low temperatures. During further cooling down to −25 °C and subsequent heating, virtually no changes of the X-ray diffraction pattern were recorded up to 20 °C. Above this temperature, a reverse transition from orthorhombic to cubic structure took place. A narrow peak, characteristic for cubic phase, appeared at 40 °C and remained unchanged on heating to 100 °C and subsequent cooling to 17 °C. Similar behavior was observed for $Li_{1.005}Mn_{1.995}O_4$ sample (Fig. 2b). In Fig. 3, together with the conductivity of the stoichiometric spinel and Li substituted spinel, the FWHM of the 4 0 0 reflection is also plotted as a function of temperature. The temperature interval in which values of the conductivity and the FWHM were different on cooling and on heating is marked by dotted vertical lines. As can be seen in Fig. 3, the thermal hysteresis of the FWHM was well correlated with the thermal hysteresis of conductivity. In the stoichiometric $LiMn_2O_4$ the thermal hysteresis of the conductivity and of the FWHM of 4 0 0 reflection extends over wider temperature interval than in the lithium-substituted spinel $Li_{1.005}Mn_{1.995}O_4$.

The sample prepared from powder supplied by Alfa-Aesar and heat-treated at 800 °C, similarly as the samples synthesized by sol–gel technique, exhibited phase transition from cubic to orthorhombic structure upon cooling below room temperature (Fig. 4a). Structural transition, clearly visible in the X-ray pattern as splitting of the 4 0 0 reflection, was accompanied by a decrease of conductivity by a factor of about 10. The thermal hysteresis of conductivity was well correlated with the hysteresis of the FWHM of the 4 0 0 reflection (Fig. 5a), however, it extended over narrower interval of temperature than in the case of samples prepared by the sol–gel method.

In the case of sample prepared from powder supplied by Sigma–Aldrich and heat-treated at 800 °C, there was no step-wise change of conductivity observed upon cooling or heating in the temperature range between 100 and −25 °C (Fig. 5b). The FWHM of the 4 0 0 reflection increased only slightly upon cooling from 100 to −25 °C. There was no indication of thermal hysteresis neither the conductivity nor the FWHM. Although the phase transition was not detected in the conductivity measurements, the X-ray pattern measured with the position sensitive detector indicated pure cubic phase above room temperature, while at low temperatures there was some broadening of the 4 0 0 reflection and an increased intensity around 43.7° (2θ), between the 4 0 0 maximum and the 1 1 1 reflection from the Cu film serving as electrode. The Rietveld analysis of the X-ray diffraction pattern, measured in the Bragg–Brentano geometry at −25 °C, indicated a mixture of two coexistent phases: cubic and orthorhombic. Contributions of the two phases to the diffraction pattern near the 4 0 0 reflection of the cubic phase are presented in Fig. 6. Thus the phase transition from cubic to orthorhombic structure was in progress but not complete even after cooling to −25 °C.

The results of Rietveld refinement of the X-ray patterns of the studied samples are summarized in Table 1. Single lattice
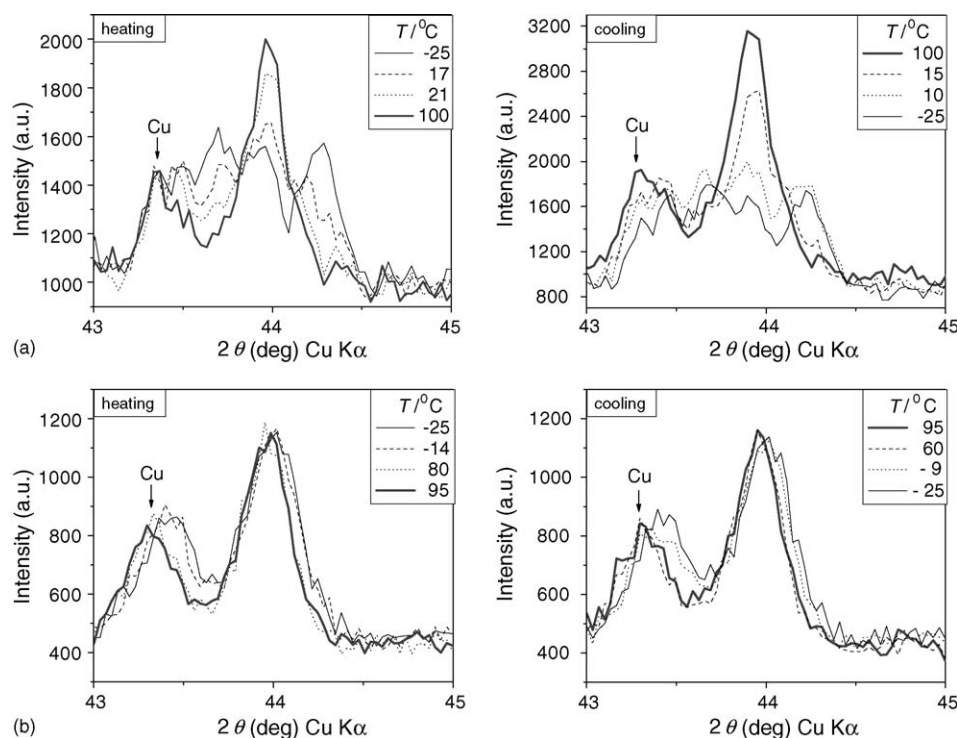
Fig. 4. XRD pattern near the 4 0 0 reflection recorded at various temperatures during heating and cooling of pellets prepared from powders supplied by: (a) Alfa-Aesar; (b) Sigma–Aldrich.

constant of cubic phase is given for patterns measured above room temperature at +50 °C (or +25 °C). For the orthorhombic phase present at low temperature (measurement at −25 or −4 °C), Table 1 gives the lattice constant a (of the medial value) and the difference between the largest and the smallest lattice constants $b − c$. As can be seen, value of the $b − c$ difference is between 0.0726 and 0.0854 Å for all investigated samples, indicating similar extent of the orthorhombic distortion. The phase analysis based on the Rietveld refinement proved that the samples prepared from powders obtained by sol–gel method and heat treated at 800 °C are single phase (cubic above room temperature, orthorhombic below 0 °C). The lattice constant of the cubic phase of the lithium substituted spinel $Li_{1.005}Mn_{1.995}O_4$ is slightly smaller than that of the stoichiometric spinel $LiMn_2O_4$, in agreement with the dependence of the lattice constant on composition for the series of solid solutions $Li_{1+x}Mn_{2−x}O_4$ [24,25].

According to the phase analysis by Rietveld refinement, powder supplied by Alfa-Aesar contained Mn_3O_4 as an impurity phase, whose content decreased from 3% to 1% in course of annealing at 800 °C. After annealing the lattice constant of the cubic spinel phase is larger than in powder as received, which indicates that the molar ratio of manganese to lithium increased as result of incorporation of manganese from the impurity oxide Mn_3O_4. Powder supplied by Sigma–Aldrich contained Li_2MnO_3 as an impurity phase, whose content was about 5% and decreased to 3.5% upon heat-treatment at 800 °C. The lattice constant of the cubic spinel, which is the major phase above room temperature, did not change significantly as a result of annealing, thus no changes of the spinel phase composition can be evidenced. The phase analysis of the X-ray diffraction patterns

measured at −25 °C for the powder supplied by Sigma–Aldrich showed coexistence of the orthorhombic and cubic phases. The calculated weight fraction of the two phases indicated that the content of the cubic phase at −25 °C remained higher in the powder annealed at 800 °C than in the powder as received. However, it is worth noting that the results of phase analysis by means of the Rietveld profile refinement should be treated with caution, since the anisotropy of additional phases can cause overestimation of their fraction in the system, as demonstrated by Massarotti et al. for an analogous case of the coexistent phases: $LiMn_2O_4$ and Li_2MnO_3 [26]. Furthermore, the weight fractions of the cubic and orthorhombic spinel phases, obtained by Rietveld refinement of the XRD profiles measured at −25 °C for powder supplied by Sigma–Aldrich, seem to indicate evolution of phase content resulting from annealing, which is in disagreement with the results of impedance measurements extended down to −65 °C. As can be seen in Fig. 7b, the measured conductivity showed a deviation from the Arrhenius type linear dependence of the logarithm of conductivity on the inverse temperature in the case of the Sigma–Aldrich sample sintered at 800 °C, whereas presence of such deviation is not evident for the sample prepared from powder as received. As a matter of fact, the conductivity of samples, which are pressed from powder as received, is above room temperature roughly an order of magnitude lower than conductivity of samples sintered at 800 °C, for samples supplied by Alfa-Aesar as well as by Sigma–Aldrich. The difference of conductivity is likely to be due to poor contact between crystallites in pressed samples, which becomes vastly improved by sintering, thus removing constrictions to current flow. Nevertheless, the decrease of conductivity as a result of the phase
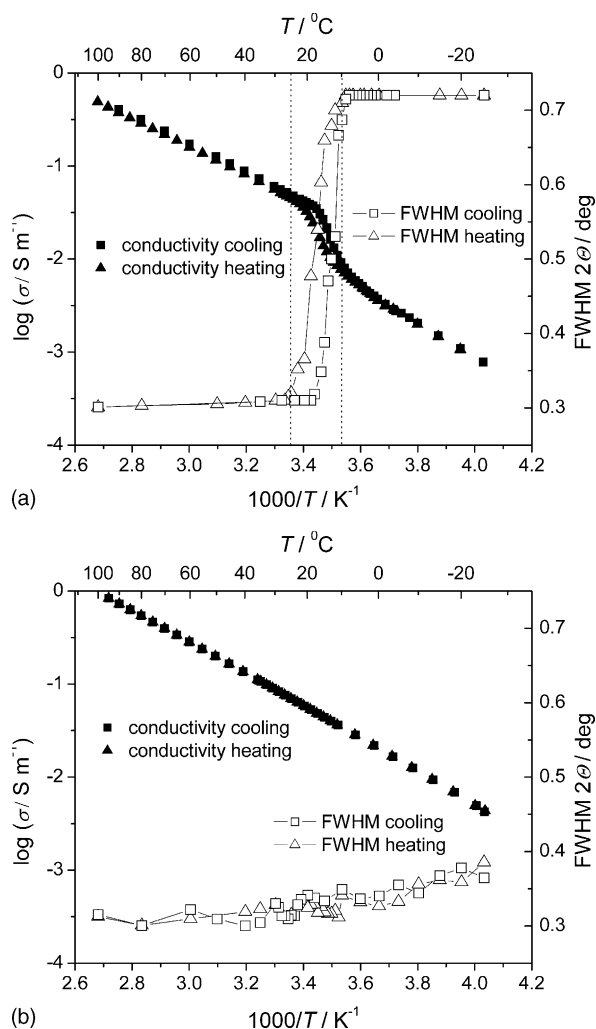
Fig. 5. Temperature dependence of the conductivity and the full width at half maximum (FWHM) of the 4 0 0 reflection for spinel samples prepared from powders supplied by: (a) Alfa-Aesar; (b) Sigma–Aldrich. Measurements on pellets sintered at 800 °C.
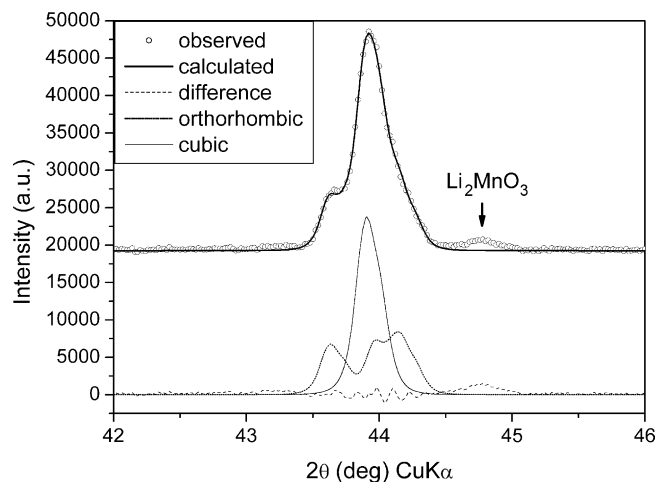

Fig. 6. Portion of the X-ray diffraction pattern, observed in the standard Bragg–Brentano geometry at −25 °C, of powder supplied by Sigma–Aldrich and heat-treated at 800 °C (upper curve, circles). Solid line is the fitted profile calculated taking into account coexistence of cubic and orthorhombic spinel phases. Curves with baseline at zero intensity show contributions to the fitted profile from cubic and orthorhombic phases as well as the difference between observed and calculated patterns. Calculated curves were generated by single peak analysis (PeakFit) in agreement with the Rietveld refinement of the full profile (Fullprof). Contribution of the impurity phase Li_2MnO_3 was not included in single peak analysis.

transition is clearly seen below room temperature in case of the sample pressed from Alfa-Aesar powder, while the conductivity of sample pressed from Sigma–Aldrich powder exhibits a slight opposite effect if any (Fig. 7).

Effect of the phase transition on the conductivity can be better revealed by comparing the conductivity measured at low temperatures with the conductivity calculated by extrapolation of the Arrhenius dependence fitted to the conductivity data measured above room temperature, see dashed straight lines in Fig. 7. Magnitude of the deviation from the Arrhenius dependence may be quantified by the ratio of the conductivity measured at −60 °C

Table 1
Crystal structure and phase content of the studied materials

Sample	T (°C)	Spinel phases	Lattice constant a (Å)	Difference $b-c$ (Å)	Bragg R-factor	Fraction (%)	Additional phases	Fraction (%)
LiMn$_2$O$_4$ sol–gel annealed 800 °C	25	Cubic	8.2475(2)	0	2.9	100	None	–
	−4	Orthorhombic	8.2537(2)	0.0785(3)	5.1	100		
Li$_{1.005}$Mn$_{1.995}$O$_4$ sol–gel annealed 800 °C	25	Cubic	8.2448(5)	0	3.8	100	None	–
	−4	Orthorhombic	8.2505(3)	0.0765(5)	5.1	100		
LiMn$_2$O$_4$ Alfa-Aesar as received	50	Cubic	8.2408(6)	0	15.4	96.9	Mn$_3$O$_4$	3.1
	−25	Orthorhombic	8.2417(9)	0.0726(13)	13.6	96.9		
LiMn$_2$O$_4$ Alfa-Aesar annealed 800 °C	50	Cubic	8.2539(6)	0	9.1	99.0	Mn$_3$O$_4$	1.0
	−25	Orthorhombic	8.2554(9)	0.0854(13)	9.6	99.0		
LiMn$_2$O$_4$ Sigma–Aldrich as received	50	Cubic	8.2433(7)	0	7.6	95.1	Li$_2$MnO$_3$	4.9
	−25	Orthorhombic	8.2423(5)	0.0844(7)	11.5	62.7		
	−25	Cubic	8.2379(7)	0	8.1	32.4		
LiMn$_2$O$_4$ Sigma–Aldrich annealed 800 °C	50	Cubic	8.2446(5)	0	8.6	96.5	Li$_2$MnO$_3$	3.5
	−25	Orthorhombic	8.2409(5)	0.0837(7)	13.1	49.7		
	−25	Cubic	8.2451(7)	0	10.2	46.8		

For orthorhombic phase the lattice constant a (of the medial value) and difference between the largest and the smallest lattice constants $b-c$ are given.
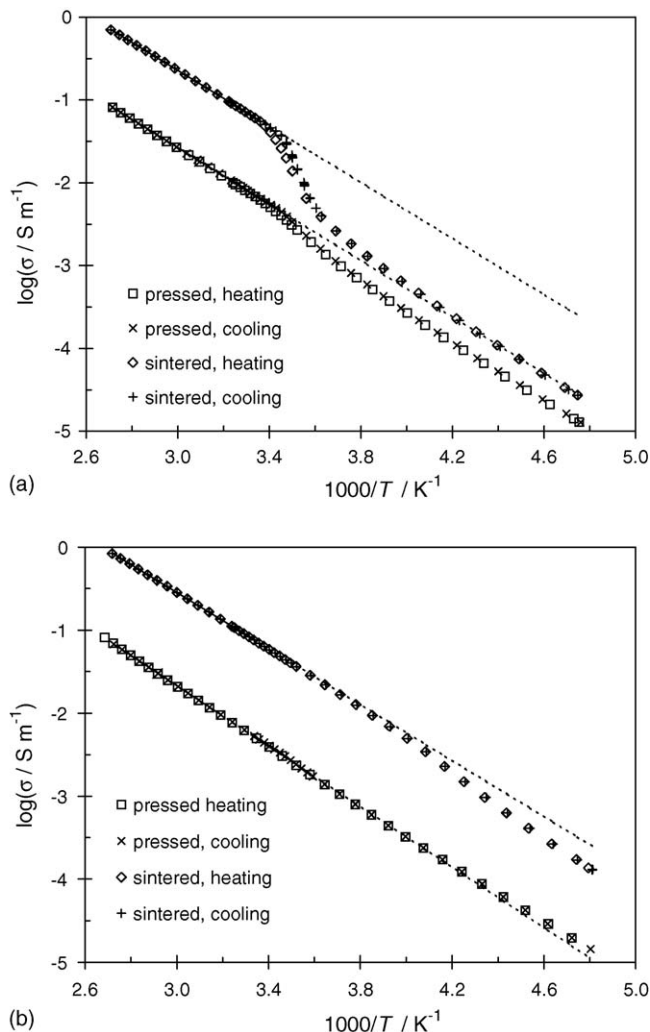
Fig. 7. Temperature dependence of conductivity of samples prepared from powders supplied by: (a) Alfa-Aesar; (b) Sigma–Aldrich. Conductivity of pellets pressed from powders as received is compared with that of pellets subsequently sintered at 800 °C. Dashed straight lines are calculated based on the Arrhenius dependence fitted to the data measured above room temperature during cooling.

Table 2
Crystallite size based on the integral width of the 2 2 2 X-ray reflection and average grain size calculated as average distance between grain boundaries on SEM picture for spinel samples heat-treated at 800 °C

Sample	Crystallite size (nm)	Grain size (μm)
$LiMn_2O_4$ (sol–gel)	42	0.7
$Li_{1.005}Mn_{1.995}O_4$ (sol–gel)	44	0.7
$LiMn_2O_4$ (Alfa-Aesar)	41	1.4
$LiMn_2O_4$ (Sigma–Aldrich)	44	1.1

In the case of samples sintered at 800 °C from powders synthesized by the sol–gel method, the ratio of the measured to extrapolated conductivity at −60 °C was 0.04 for $LiMn_2O_4$ and 0.07 for $Li_{1.005}Mn_{1.995}O_4$, calculated based on measurements presented in [18]. Smaller values of the considered ratio in the case of sol–gel synthesized samples indicate larger effect of the phase transition on the conductivity than observed in samples prepared from commercially available powders.

The average crystallite sizes, as estimated from the full width at half maximum of the 2 2 2 reflection of cubic spinel, are very similar for all studied samples, see Table 2, and equal about 40 nm. Similar values of the average crystallite size were estimated for the orthorhombic phase. However, the SEM micrographs of fractured pellets, Fig. 1, clearly show that the average grain size of the sintered samples prepared from powders obtained by sol–gel method is smaller than the grain size of pellets sintered from commercially available powders. Estimated values of grain size, given in Table 2, are of the order of 1 μm.

The average crystallite size, calculated from the width of X-ray diffraction peak, should be more precisely interpreted as the size of areas of coherent diffraction in polycrystalline material and should not be confused with grain size. Present findings that the areas of coherent scattering have similar size in the four studied samples heat-treated at 800 °C, irrespective of the origin of $LiMn_2O_4$ powder and despite differences in the grain size (as observed by SEM), indicate that the crystal structure of lithium manganese oxide spinel does not conform to perfect translational symmetry. Both the cubic phase and the orthorhombic phase appear to exhibit a mosaic domain structure of nanometric size, which is more than an order of magnitude smaller than the average size of grains observed by SEM. The imperfect crystal structure may be a result of the structural phase transition from cubic to orthorhombic symmetry.

The magnitude of conductivity change accompanying the phase transition from cubic to orthorhombic structure seems to depend on the presence of impurity phases. The decrease of Li_2MnO_3 fraction in the Sigma–Aldrich sample, caused by heat-treatment at 800 °C, coincided with appearance of a decrease of conductivity during the phase transition, which was not observed for the sample pressed from powder as received. A distinctive enhancement of the conductivity anomaly was observed for Alfa-Aesar sample, in which the fraction of the additional phase Mn_3O_4 was reduced by heat-treatment. Plausible explanation for this phenomena is change of the actual stoichiometry of the spinel phase, which is known to influence the course of phase transition [5,7,14–16]. The presence of additional phases may

to value of the conductivity calculated for this temperature by extrapolation. Value of this ratio was 0.5 for the sample sintered at 800 °C from powder supplied by Sigma–Aldrich, while for the sample sintered from powder supplied by Alfa-Aesar this ratio was 0.11. Incidentally, this ratio was equal 0.5 for the sample prepared from Alfa-Aesar powder as received, however, this sample exhibited deviation from the Arrhenius dependence of conductivity already below 15 °C, similarly as the sample sintered at 800 °C (Fig. 7a). The larger change of conductivity accompanying the phase transition in the sintered sample may be related to the larger extent of the orthorhombic distortion as evidenced by values of the difference between the extreme values of lattice constant $c - b$ given in Table 1. In the case of sample sintered at 800 °C from Sigma–Aldrich powder, deviation from the Arrhenius dependence was seen only below −25 °C, indicating that the phase transition was shifted to lower temperatures. Thus at −25 °C coexistence of cubic and orthorhombic phases was expected as confirmed by the X-ray diffraction pattern (Fig. 6).

also disturb the local environment, introducing charge disorder into the orthorhombic structure and preserving easy conductivity pathways. Conductivity is also influenced by evolution of the microstructure during sintering, which improves contact between grains. It appears that variation of the pattern of temperature dependence of conductivity in the studied system has quite complex origin. Further investigation is required to determine, which of the factors mentioned above plays the dominant role in altering the course of phase transition and its effect on the electrical conductivity.

4. Conclusions

Samples prepared from powders obtained by sol–gel method as well as from powder supplied by Alfa-Aesar and heat-treated at 800 °C exhibit phase transition from cubic to orthorhombic structure upon cooling below room temperature. In the course of phase transformation, the changes of the full width at half maximum of the 4 0 0 X-ray reflection were well correlated with the changes of conductivity. The observed decrease of conductivity during phase transition depends on the method of spinel preparation. The phase transition was not complete even at −25 °C in the sample prepared from powder supplied by Sigma–Aldrich and no stepwise change of conductivity was observed for this sample. Additional impurity phases were found and characterized in commercial samples, whereas the samples prepared by sol–gel method were single phase after heat-treatment at 800 °C. It can be deduced that presence of the impurity phases, especially Li_2MnO_3 detected in powder supplied by Sigma–Aldrich, suppresses the phase transition of the lithium manganese spinel from cubic to orthorhombic symmetry. Heat-treatment of the commercial samples reduced the amount of impurity phases and enhanced the effect of phase transition upon conductivity.

Although the present results do not provide any direct information on the performance of the studied lithium manganese oxide spinels as cathode in lithium-ion battery, they imply caution when using lithium manganese oxide spinel from commercial suppliers for development of lithium-ion batteries, since presence of impurity phases may cause deviation from stoichiometry and affect electrical properties of the spinel phase, leading to unexpected performance of the cathode.

Acknowledgements

References

[1] M.M. Thackeray, W.I.F. David, P.G. Bruce, J.B. Goodenough, Mater. Res. Bull. 18 (1983) 461.
[2] J.B. Goodenough, M.M. Thackeray, W.I.F. David, P.G. Bruce, Rev. Chim. Miner. (1984) 435.
[3] J.M. Tarascon, D. Guyomard, J. Electrochem. Soc. 138 (1991) 2864.
[4] J.B. Goodenough, A. Manthiran, B. Wnetrzewski, J. Power Sources 43/44 (1993) 269.
[5] A. Yamada, J. Solid State Chem. 122 (1996) 160.
[6] H. Yamaguchi, A. Yamada, H. Uwe, Phys. Rev. B 58 (1998) 8.
[7] Y. Shimakawa, T. Numata, J. Tabuchi, J. Solid State Chem. 131 (1997) 138.
[8] K. Oikawa, T. Kamiyama, F. Izumi, B.C. Chakoumakos, H. Ikuta, M. Wakihara, J. Li, Y. Matsui, Solid State Ionics 109 (1998) 35.
[9] J. Rodriguez-Carvajal, G. Rousse, C. Masquelier, M. Hervieu, Phys. Rev. Lett. 81 (1998) 4660.
[10] G. Rousse, C. Masquelier, J. Rodriguez-Carvajal, M. Hervieu, Electrochem. Solid State Lett. 2 (1999) 6.
[11] G. Rousse, C. Masquelier, J. Rodriguez-Carvajal, E. Elkaim, J.-P. Lauriat, J.L. Martinez, Chem. Mater. 11 (1999) 3629.
[12] K. Świerczek, J. Marzec, M. Marzec, J. Molenda, Solid State Ionics 157 (2003) 89.
[13] R. Dziembaj, M. Molenda, J. Power Sources 119–121 (2003) 121.
[14] J. Sugiyama, T. Atsumi, A. Koiwai, T. Sasaki, T. Hioki, S. Noda, N. Kamegashira, J. Phys. Condens. Matter. 9 (1997) 1729.
[15] R. Kanno, M. Yonemura, T. Kohigashi, Y. Kawamoto, M. Tabuchi, T. Kamiyama, J. Power Sources 97/98 (2001) 423.
[16] M. Tachibana, T. Tojo, H. Kawaji, T. Atake, M. Yonemura, R. Kanno, Phys. Rev. B 68 (2003) 094421.
[17] D. Lisovytskiy, Z. Kaszkur, N.V. Baumer, J. Pielaszek, M. Molenda, R. Dziembaj, J. Marzec, J. Molenda, J. Dygas, M. Kopeć, F. Krok, Mol. Phys. Rep. 35 (2002) 26.
[18] J.R. Dygas, M. Kopeć, F. Krok, D. Lisovytskiy, J. Pielaszek, Solid State Ionics 176 (2005) 2153.
[19] D. Lisovytskiy, Z. Kaszkur, J. Pielaszek, M. Marzantowicz, J.R. Dygas, Solid State Ionics 176 (2005) 2059.
[20] R. Dziembaj, M. Molenda, D. Majda, S. Walas, Solid State Ionics 157 (2003) 81.
[21] J. Rodriguez-Carvajal, T. Roisnel, Fullprof 98 and WinPLOTR, International Union for Crystallography, Newsletter No. 20, 1998. http://www-llb.cea.fr/fullweb/winplotr/winplotr.htm.
[22] J.R. Dygas, P. Kurek, M.W. Breiter, Electrochim. Acta 40 (1995) 1545.
[23] M. Marzantowicz, J.R. Dygas, F. Krok, A. Łasińska, Z. Florjańczyk, E. Zygadło-Monikowska, Electrochim. Acta 51 (2006) 1713.
[24] P. Endres, B. Fuchs, S. Kemmler-Sack, K. Brandt, G. Faust-Becker, H.-W. Praas, Solid State Ionics 89 (1996) 221.
[25] Y. Gao, J.R. Dahn, J. Electrochem. Soc. 143 (1996) 1783.
[26] V. Massarotti, D. Capsoni, M. Bini, C.B. Azzoni, A. Paleari, J. Solid State Chem. 128 (1997) 80.